

Equilibrium of a non-neutral plasma in a toroidal magnetic shear configuration

Haruhiko Saitoh,^{a)} Zensho Yoshida,^{b)} and Chihiro Nakashima^{c)}
The University of Tokyo, Bunkyo-ku, Tokyo 113-0033, Japan

(Received 11 July 2001; accepted for publication 8 October 2001)

The conventional rigid rotation model of thermal equilibrium does not apply to a toroidal non-neutral plasma trap; the nonuniformity of the magnetic field produces an inhomogeneous flow. For sufficiently large ω_c/ω_p (ω_c : cyclotron frequency; ω_p : plasma frequency), the flow can be approximated by the $\mathbf{E}\times\mathbf{B}$ drift velocity. The toroidal equilibrium of an electron plasma has been analyzed for a rather complex geometry of magnetic shear configuration. © 2002 American Institute of Physics. [DOI: 10.1063/1.1426229]

I. INTRODUCTION

There is an increasing interest in diverse applications of non-neutral plasmas; traps of charged particles (including antimatters)¹ play an essential role in nuclear and atomic physics experiments, as well as in many different applications such as medical and maternal diagnostics. The self-electric field and the resultant strong flow are also applied to the study of both nonlinear vortex dynamics and various types of structure formations. Recently, the self-organization of a strong diamagnetic (high-beta) state was predicted by a two-fluid model.² Studies on these non-neutral (or strong flow) systems may open up an innovative path toward the advanced fusion concept.

Toroidal systems have advantages in trapping high energy, high density charged particles, or multiple species of different charges, because they do not use external electric fields to plug open magnetic-field lines.³⁻⁸ The Proto-RT (Proto-type Ring Trap) device, shown in Fig. 1, was constructed to study various physical phenomena in toroidal nonneutral plasmas.⁹ Proto-RT can operate with a variety of magnetic-field configurations, which are generated by two kinds of poloidal field coils (an internal conductor coil and two vertical field coils) in addition to toroidal field coils. This system enables us to test innovative concepts, such as particle injection across magnetic surfaces^{10,11} and plasma stabilization by the effect of magnetic shear.¹²

In Proto-RT, electrons are injected by an electron gun placed near the magnetic separatrix. In the peripheral region, electrons trace chaotic orbits, and strong randomization causes effective spreading of the beam (Fig. 2). Because of the long orbits of chaotic motion, nonadiabatic effects yield diffusion toward the confinement region.⁹ Thermalized electrons generate a macroscopic equilibrium. In this article, we study the structure of the non-neutral plasma equilibrium in a toroidal device of the Proto-RT type. The plasma shows

paramagnetism being confined to the strong magnetic-field side of the torus.

II. EQUILIBRIUM MODEL AND METHOD OF CALCULATIONS

For a low-density magnetized non-neutral plasma ($\omega_c/\omega_p \gg 1$, ω_c : cyclotron frequency; ω_p : plasma frequency), we can use the $\mathbf{E}\times\mathbf{B}$ approximation of the flow velocity.³

$$\mathbf{v} = -\frac{\nabla\phi \times \mathbf{B}}{B^2}, \quad (1)$$

where ϕ is the electrostatic potential. The continuity equation in a steady state reads

$$\nabla \cdot (n\mathbf{v}) = -\left[\nabla\phi \times \nabla\left(\frac{n}{B^2}\right) \right] \cdot \mathbf{B} = 0. \quad (2)$$

Here, n is the number density of charged particles. When the magnetic field \mathbf{B} has a component perpendicular to $\nabla\phi$, Eq. (2) demands

$$\nabla\phi \times \nabla\left(\frac{n}{B^2}\right) = 0. \quad (3)$$

This condition applies for an axisymmetric toroidal device with a toroidal magnetic field. Equation (3) implies that

$$n = B^2 f(\phi), \quad (4)$$

where f is a certain smooth function of ϕ .

The n and ϕ must also satisfy the Poisson equation

$$\nabla^2\phi = -\frac{qn}{\epsilon_0} \quad (5)$$

with boundary conditions (q is the charge, ϵ_0 is the vacuum dielectric constant). We can replace the boundary condition by the corresponding image charge ρ_i induced on the conductor walls. The total charge in the system is given by $\rho = qn + \rho_i$. We decompose $\phi = \phi_p + \phi_i$ imposing

$$\nabla^2\phi_p = -\frac{qn}{\epsilon_0} = -\frac{qB^2}{\epsilon_0} f(\phi), \quad (6)$$

^{a)}Graduate School of Frontier Sciences; electronic mail: saito@plasma.q.t.u-tokyo.ac.jp

^{b)}Graduate School of Frontier Sciences.

^{c)}Graduate School of Engineering.

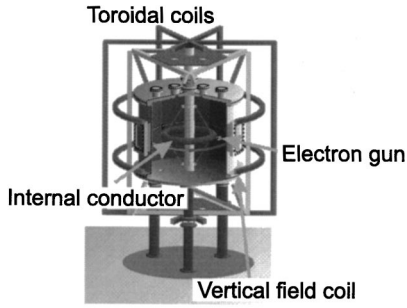


FIG. 1. Proto-RT. A toroidal non-neutral plasma confinement device, capable of generating various kinds of magnetic-field configurations.

$$\nabla^2 \phi_i = -\frac{\rho_i}{\epsilon_0} \quad (7)$$

with the homogenized boundary condition $\phi_p|_{\infty} = \phi_i|_{\infty} = 0$.

Equation (6) is integrated as

$$\phi_p(\mathbf{r}) = \frac{q}{4\pi\epsilon_0} \int_{-\infty}^{\infty} \frac{B^2 f(\phi)}{|\mathbf{r}-\mathbf{r}'|} d\mathbf{r}'. \quad (8)$$

For an axisymmetric toroidal plasma, Eq. (8) reads in the cylindrical coordinate (r, θ, z) ,

$$\begin{aligned} \phi_p(\mathbf{r}) &= -\frac{e}{4\pi\epsilon_0} \\ &\times \int \int \int \frac{B(\mathbf{r}')^2 f[\phi(\mathbf{r}')] r' dr' d\theta' dz'}{r^2 + r'^2 + (z-z')^2 - 2rr' \cos \theta'} \\ &= \frac{e}{4\pi\epsilon_0} \int \int B(\mathbf{r}')^2 f[\phi(\mathbf{r}')] A(\mathbf{r}, \mathbf{r}') dr' dz'. \end{aligned} \quad (9)$$

The kernel $A(\mathbf{r}, \mathbf{r}')$ is defined by

$$A(\mathbf{r}, \mathbf{r}') = \frac{k}{2} \sqrt{\frac{r'}{r}} K(k),$$

where $K(k)$ is the complete elliptic integral of the first kind:

$$K(k) = \frac{k^2}{2} \int_0^{\pi/2} \frac{d\theta}{\sqrt{1-k^2 \sin^2 \theta}},$$

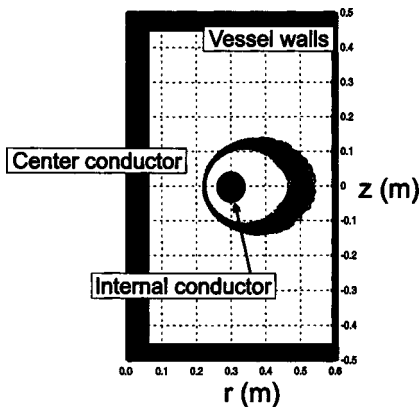


FIG. 2. Typical orbits (projected onto a poloidal cut) of electrons in Proto-RT. The electrons are injected by an electron gun located at $r=49$ cm.

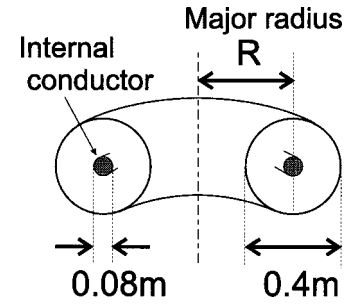


FIG. 3. Simple model of toroidal internal conductor device. Changing the major radius R , we examine the toroidal effect (Figs. 4 and 5).

$$k^2 = \frac{4rr'}{(r+r')^2 + (z-z')^2}.$$

For the image charge, we integrate Eq. (7) in a similar form:

$$\phi_i(\mathbf{r}) = \frac{1}{4\pi\epsilon_0} \int_{-\infty}^{\infty} \frac{\rho_i(\mathbf{r}')}{|\mathbf{r}-\mathbf{r}'|} d\mathbf{r}'. \quad (10)$$

The image charge ρ_i and the corresponding potential ϕ_i are determined by the boundary condition. When the wall conductors are grounded (e.g.), we impose

$$\phi = \phi_p + \phi_i = 0 \quad (11)$$

on the boundary. In the calculations, we use delta-measure image charges distributed on the conducting walls. The boundary condition is examined at the same number of points on the conductors, and the image charges are adjusted to satisfy Eq. (11).

III. STRUCTURE OF A TOROIDAL NON-NEUTRAL PLASMA EQUILIBRIUM

The method given in the previous section is applicable to rather complex magnetic-field configurations and vessel shapes. We consider an electron plasma in a toroidal device in which a dipole magnetic field is generated by an internal conductor. Combining vertical and toroidal fields, a variety of magnetic-field configurations can be created. The structure of an electron plasma and its control methods in such configurations are discussed in this section.

A. Paramagnetic equilibrium of a toroidal non-neutral plasma

In the present $\mathbf{E} \times \mathbf{B}$ drift model of equilibrium, the plasma density concentrates in a preferential high-magnetic field region (a kind of paramagnetism). Hence, the plasma shifts inward in a toroidal device. The particle injection method of Proto-RT arranges a particle source in a weak-field place. The confinement region and the particle source can be naturally separated.

When a magnetized electron moves with an $\mathbf{E} \times \mathbf{B}$ drift speed that is inversely proportional to the magnetic-field strength B , the electron spends a longer time in a region of larger B . Hence, the plasma shows "paramagnetism." When a toroidal magnetic field is applied, and consequently the velocity of an electron has a poloidal component, electron distribution will shift inward, because the toroidal field has a

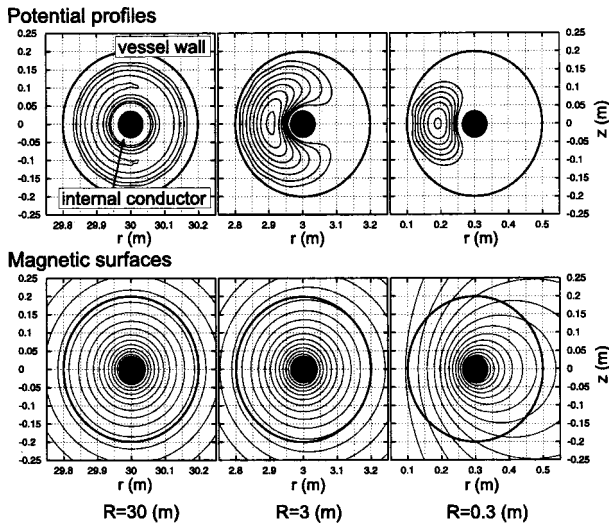


FIG. 4. Potential profiles and magnetic surfaces in a poloidal cross section of toroidal devices with different major radii (see Fig. 3). Electrostatic potentials on both boundaries of vessel walls and internal conductor are assumed to be zero. A magnetic field is generated mainly by an internal conductor, and a weak toroidal magnetic field is also applied.

$1/r$ profile (r : radius from the axis of the torus). Superposition of poloidal fields modifies the field distribution and hence modifies the density profile.

To overview the basic property of equilibrium, we have studied solutions in circular domains of a poloidal cross section with some different aspect ratios (Fig. 3). Figure 4 shows the potential profiles when the magnetic field is generated mainly by an internal conductor. The function f in Eq. (4) is assumed to be a linear function of the potential ϕ . For typical number density of the plasma $n = 10^{11} \text{ m}^{-3}$ and typical magnetic-field strength $B = 10^{-2} \text{ T}$, $\omega_c/\omega_p \sim 10^2$ and $L/\lambda_D \sim 10^1$ (L : typical length of the plasma; λ_D : Debye length). When the aspect ratio of the device is large, the magnetic field is approximately uniform, and the potential profile becomes almost symmetric in the $r-z$ plane. In this case, electrons describe helical drift orbits circulating around the internal conductor with almost constant velocity. For a small aspect ratio, the nonuniformity of the magnetic field becomes strong, and the plasma shifts inward due to the paramagnetism.

The other reason why the equilibrium density shifts inward is the effect of image charges on the boundary.¹³ In Fig. 5, we assume an artificial homogeneous magnetic-field strength in order to examine this effect. The toroidal curva-

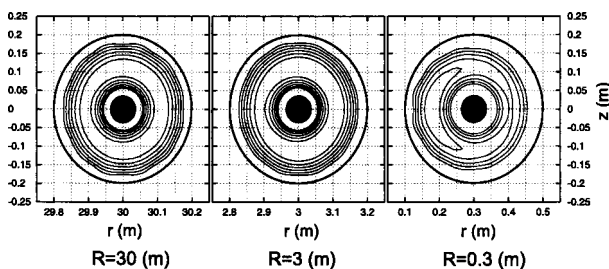


FIG. 5. Potential profiles in artificial homogeneous magnetic fields. The other conditions, except for the magnetic-field strength, are the same as those in Fig. 4.

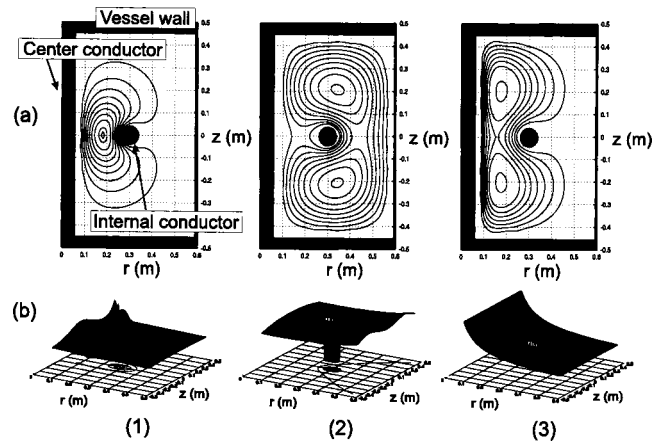


FIG. 6. Control of equilibrium by magnetic field. (a) Potential profiles in the Proto-RT device. (b) Profiles of the magnetic-field strength. (1) Dipole magnetic field plus toroidal field, (2) vertical field plus toroidal field, and (3) only toroidal field.

ture proceeds as a hoop force. When the plasma shifts inward, this force can be cancelled by an electrostatic drag force generated by the image charges on the conductors.

B. Position and shape control

One of the advantages of a toroidal internal-conductor trap stems from its high degree of freedom to control the plasma. By changing magnetic field and boundary potentials, we can produce a variety of equilibria.

The position and shape of the toroidal plasma equilibrium can be controlled by changing the magnetic field and also by applying external electric fields with changing the boundary potentials. We tested these effects in the geometry of Proto-RT. Figure 6 shows equilibria in three different types of magnetic fields. The potential profiles show paramagnetism, as mentioned in Sec. II A, while the structures are more complicated because of realistic field configurations and the device geometry of the Proto-RT device. [The function f of Eq. (4) and plasma parameters are the same as in Sec. III A.] We observe the strong influence of the image charges on the internal conductor. The image charges, having the opposite sign of the plasma charge, diminish the space potential near the conductor. If the magnetic field is not

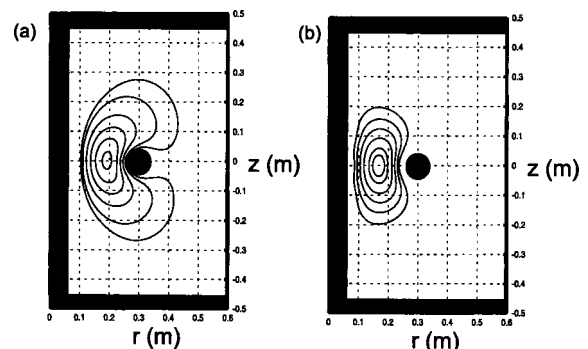


FIG. 7. Control of equilibrium by external electric field. The applied potentials on the center conductors are (a) $+\phi_{\text{max}}/10$ and (b) $-\phi_{\text{max}}/10$, where ϕ_{max} is the maximum potential inside the plasma. The magnetic field is same as that in Fig. 6(1).

strong enough on the equatorial plane of the device, the profile of plasma separates into two peaks. Because the guiding center of particles parallels the level sets of the potential, the particles are divided into two groups.

The boundary condition of the potential can be changed by biasing the internal conductor and/or a certain part of the vessel. This degree of freedom provides us to other parameters necessary to control the equilibrium. In Fig. 7, we observe that the equilibrium is strongly influenced by a relatively small change of the boundary potentials (1/10 of the maximum potential of the plasma). This method may be useful in optimizing the stability and confinement of the plasma.

ACKNOWLEDGMENTS

The authors are grateful to Mr. Shuichi Ohsaki for discussions and suggestions. This work was supported by a Grant-in-Aid for Scientific Research from the Japanese Ministry of Education, Science, Sports and Culture No. 09308011, and by the Toray Science Foundation.

- ¹C. M. Surko, M. Leventhal, and A. Passner, *Phys. Rev. Lett.* **62**, 901 (1989).
- ²S. M. Mahajan and Z. Yoshida, *Phys. Rev. Lett.* **81**, 4863 (1998); Z. Yoshida, S. M. Mahajan, S. Ohsaki, M. Iqbal, and N. Shatashvili, *Phys. Plasmas* **8**, 2125 (2001).
- ³J. D. Daugherty and R. H. Levy, *Phys. Fluids* **10**, 155 (1967).
- ⁴J. D. Daugherty, J. E. Eninger, and G. S. Janes, *Phys. Fluids* **12**, 2677 (1969).
- ⁵G. S. Janes, *Phys. Rev. Lett.* **15**, 135 (1965).
- ⁶G. S. Janes, R. H. Levy, H. A. Bethe, and B. T. Feld, *Phys. Rev.* **145**, 925 (1966).
- ⁷P. Zaveri, P. I. John, K. Avinash, and P. K. Kaw, *Phys. Rev. Lett.* **68**, 3295 (1992).
- ⁸S. S. Khirwadkar, P. I. John, K. Avinash, A. K. Agarwal, and P. K. Kaw, *Phys. Rev. Lett.* **71**, 4334 (1993).
- ⁹Z. Yoshida *et al.*, *Nonneutral Plasma Physics III* (American Institute of Physics, New York, 1999), pp. 397–416.
- ¹⁰S. Kondoh and Z. Yoshida, *Nucl. Instrum. Methods Phys. Res. A* **382**, 561 (1996).
- ¹¹C. Nakashima and Z. Yoshida, *Nucl. Instrum. Methods Phys. Res. A* **428**, 284 (1998).
- ¹²S. Kondoh, T. Tatsuno, and Z. Yoshida, *Phys. Plasmas* **8**, 2635 (2001).
- ¹³K. Avinash, *Phys. Fluids B* **3**, 3226 (1991).